

# Stochastic Ion Channel Gating in Dendrites

Clio González Zacarías<sup>a,\*</sup>, Yulia Timofeeva<sup>b</sup>, Michael Tildesley<sup>a</sup>

<sup>a</sup>Centre for Complexity Science, University of Warwick, Coventry, United Kingdom

<sup>b</sup>Department of Computer Science, University of Warwick, Coventry, United Kingdom

---

## Abstract

Signalling in the nervous system depends on rapid changes in the potential difference across the nerve cell membranes. These signals are mainly controlled by voltage gated ion channels, which present stochastic transitions between two possibilities: open or closed. The main objective of this project was to investigate how variation in the density of stochastic ion channels influences the cell response. For this purpose, we considered a simple model of a cell, which consists of a single dendritic branch. A discrete number of voltage gated active channels for  $Na^+$ , and  $K^+$  were distributed along the cell structure, reflecting the fact that the density of the channels varies between closer and farther sections of the dendrite with respect to the soma. As it is well established, Markov chains provide realistic models for numerous stochastic processes, therefore each type of channel was modelled using a specific Markov chain model. Using the simplest model in this class: a model with either an open or closed state, we show that it is possible to find stochastic transitions in voltage along the dendrite under simulated biological parameters.

*Keywords:* Gating ion channels, Gillespie's method, Hodgkin Huxley model.

---

## 1. Introduction

The structure of a neuron can be resolved into three different sections: (i) The soma or cell body is the where the nucleus is located and the cellular machinery integrates all of the inputs of the cell to generate output; (ii) The axon conducts electrical impulses away from the soma to different neurons and other parts of the body, like muscles and glands; (iii) The dendrite is involved in receiving and integrating thousands of synaptic inputs that come from other cells, as well as in determining the extent to which an action potential is produced [Kandel et al. (2012)]. These have a highly complex branching structure and despite being discovered over a century ago, dendrites were not thoroughly studied until the early 1950s. Although it was believed that dendrites could generate active responses, much of the early work on dendritic modelling was focused on the passive properties of the cell membrane. The active response of dendrites was initially supported by dendritic recordings from cerebellar Purkinje and hippocampal pyramidal neurons and later from other types of cells [Masukawa et al. (1983)].

In general, neurons perform nonlinear operations that bringing gain amplification and positive feedback [Koch et al. (1999)]. Therefore, intrinsic random fluctuations, due to small biochemical and electrochemical changes can significantly change the whole cell response. Furthermore, many neuronal structures are very small and due to discrete signalling of some molecules, the whole structure can be affected, i.e. molecules

as voltage gated ion channels or neurotransmitters are invariably subject to thermodynamic fluctuations [Dayan et al. (1983)]. For this reason, their behaviour will have a stochastic component which may dramatically affect the general cell behaviour. Particularly, voltage gated ion channels that selectively conduct specific ions, generate stochastic responses in the dendritic membrane. These channels demonstrate stochastic transitions between the open and closed states, and changes in the membrane potential can also influence the probability of a closed channel to open [Fall et al. (2002)]. Most models of electric activity in neurons consider the collective behaviour of a large population of ion channels continuously distributed through the cell membrane, taking into account deterministic changes in macroscopic conductances.

However evidence suggests that stochastic transitions between the states of single ion channels might also have a significant influence in neuronal computations [Strassberg et al. (1993)]. Recent work by Cannon et. al. started to address the functional consequences of stochastic gating of ion channels in neurons of different morphologies. To study how the dendritic morphology might influence the neuronal response, the same density of ion channels for each cell type was considered. Cannon et. al. challenge deterministic methods by showing that when hippocampal CA1 pyramidal neuron ion channels gate deterministically, the probability of dendritic spikes is either zero or one. Whereas using stochastic methods, this probability can vary between zero and one. Fig. 1 illustrates the work of Cannon et. al, panel (A) shows the positions of the recording electrodes along the CA1 pyramidal neuron, panel (B) presents examples of action potentials<sup>1</sup> using both deterministic and

---

\*Corresponding author

Email address: C.Gonzalez-Zacarias@warwick.ac.uk (Clio González Zacarías )

---

<sup>1</sup>The action potential (AP) is the fundamental signal used for communica-

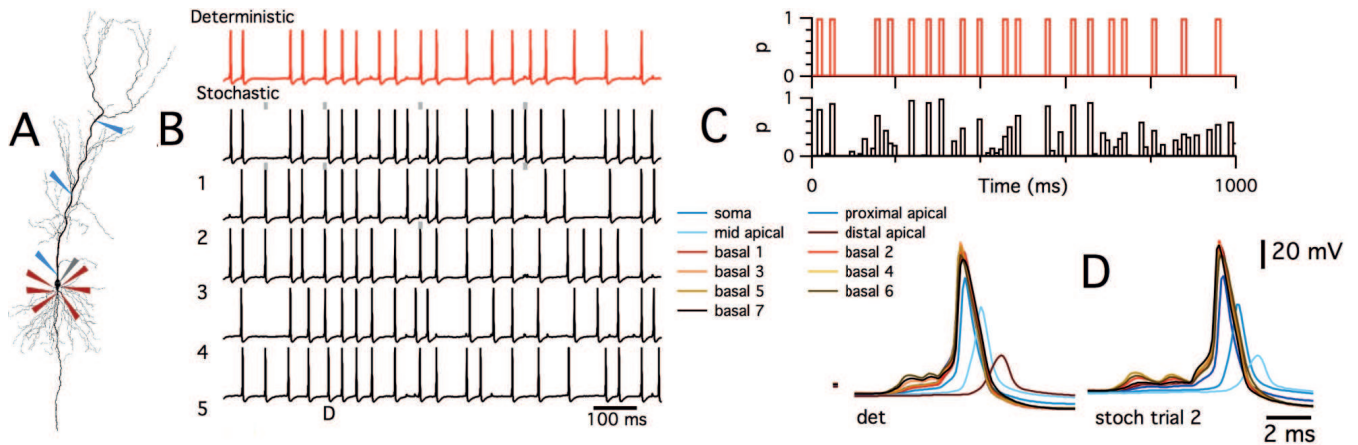


Figure 1: (A) Morphology of the simulated CA1 pyramidal neuron, illustrating positions of recording electrodes placed on the soma (grey), apical (blue) and basal (red) dendrites. (B) Examples of membrane potential responses of deterministic (red trace) and stochastic (black traces) versions of the model that describes the distributed synaptic input. Letter “D” and grey bars indicate the times of action potentials highlighted in subsequent panels. (C) Probability of somatic spike firing in 10 ms duration bins for the deterministic (red) and stochastic (black) versions of the model. (D) Examples of deterministic responses (right) and representative stochastic responses (left), for different regions in the pyramidal neuron. Figure taken from Cannon et al. (2010): “Stochastic Ion Channel Gating in Dendritic Neurons: Morphology Dependence and Probabilistic Synaptic Activation of Dendritic Spikes”

stochastic models, panel (C) shows that for stochastic methods, the probability of dendritic spike varies between zero and one. Finally, panel (D) presents the responses of different regions of the neuron using both deterministic and stochastic methods.

In the present work just the stochastic representation of gating ion channels was considered, following sections will describe this representation in more detail.

## 2. Methods

### 2.1. Ion channels

Signalling in the brain depends on the ability of nerve cells to respond to small stimuli by producing rapid changes in the membranes potential<sup>2</sup>. Ion channels are transmembrane proteins that form pores in the lipid cell membrane, facilitating the entrance or exit of ions into or out of the cell [Hille et al. (2001)]. Each cell type selects its own set of ion channels to suit its own purposes, as in the case of excitable cells, they demonstrate to be mainly permeable to sodium ( $Na^+$ ), potassium ( $K^+$ ), chloride ( $Cl^-$ ) and calcium ( $Ca^{2+}$ ). Therefore, the response of nerve cells to some stimuli is dependent on the movement of these ions (across the membrane). Nowadays, more than 100 different types of ion channel are known, each one having distinct responses to change in membrane potential, for example the soma of CA1 pyramidal neuron membrane predominantly expresses the big conductance type of  $K^+$  channels [Yuan et al. (2005)]. However, the value of the membrane potential can vary for different structures (e.g. neuronal and cardiac cells) and along the dendrites and axons, due to the non homogenous distribution of channels along the

tion within the brains neural networks.

<sup>2</sup>Membrane potential is defined as the electrical potential difference between the interior and the exterior of the cell.

cell, this can affect the neuronal response i. e. the amplitude of the action potential.

By nature of their electrostatic and chemical properties, not all the ions have the same size, for example  $K^+$  ions are larger than  $Na^+$  ions, this allows ion channels and pumps on cell membranes to be selective between different types of ions. In fact each type of channel allows only one or a few types of ions to pass i.e. if the ion channel is permeable to two type of ions, the channel will actively pump or passively allow one of the two ions to pass, while blocking the other [Hille et al. (2001)].

### 2.2. Voltage gated ion channels

Around the cell there are different kinds of ion channel, some are permanently open allowing the ions to move from both sides of the membrane. Others are activated by changes in the membrane potential allowing a fast interchange of ions between the inside and outside. This type of ion channel is called a voltage gated ion channel and they play an important role in cells of the nervous system [Kandel et al. (2012)].

It has been proposed that voltage gated channels are made of three basic parts: the voltage sensor, the pore or conducting pathway and the gate. During many years it has been assumed that conformational change modifies the shape of the channel proteins forming a small cavity used by the ions to cross through the membrane. Fig. 2-(a) represents a channel whose conformational proteins are modified in order to make the transition from a closed to an open state. The gating channels model proposes a voltage-sensing mechanism that consists of the movement of charged particles (that belong to the channel structure) within the membrane allowing the conformational change in the channel. This sensing mechanisms are known as gating particles [Sterrat et al. (2011)].

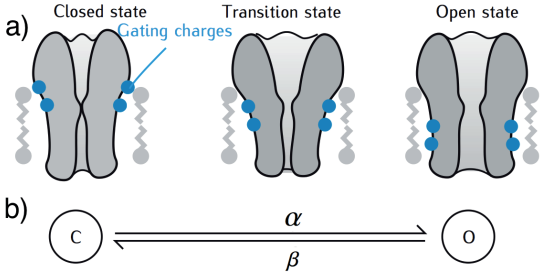
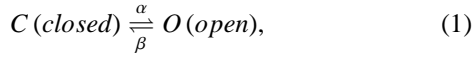


Figure 2: a) Representation of a hypothetical channel protein with two stable states: a closed state and an open state. While changing conformation between these states, the channel passes through a transition state. In each state, the gating charges (in blue) have a different position in the electric field. b) Representation of the channel as a Markov scheme. The transition state does not feature in the scheme. The opening rate is given by  $\alpha$  and the closing rate is  $\beta$ . Figure taken from Sterrat et al. (2011): *Principles of Computational Modelling in Neuroscience*.

### 2.3. Modelling channel gating as a Markov process

One way to describe the membrane excitability is to model conductance changes in terms of populations of ion channels, where each ion channel is modelled as an individual stochastic process [Strassberg et al. (1993)]. The stochastic gating of a single ion channel can be modelled as a continuous time Markov process<sup>3</sup>. The kinetic scheme for an ion channel with two states<sup>4</sup>, one closed ( $C$ ) and the other open ( $O$ ), where the parameter  $\alpha$  is the  $C \rightarrow O$  rate and  $\beta$  is the  $O \rightarrow C$  rate (both with units of milli seconds  $ms^{-1}$ ) is given by [Fall et al. (2002)]:



If  $x$  is define as a random variable (RV), with values  $x \in \{C, O\}$ . The probability that  $x$  takes one of these values at time  $t$  is  $P_O(t) = \text{Prob}[x = O, t]$  or  $P_C(t) = \text{Prob}[x = C, t]$ ; where  $P_O(t) + P_C(t) = 1$ . If the channel is closed at time  $t$ , the probability that it will open by time  $t + \Delta t$  is:

$$\text{Prob}[x = O, t + \Delta t | x = C, t] = \alpha \Delta t. \quad (2)$$

This is a conditional probability. Therefore we need to multiply by the probability that the channel is in state  $C$  at time  $t$

$$\text{Prob}[C \rightarrow O] = \text{Prob}[x = O, t + \Delta t | x = C, t] P_C(t) \quad (3)$$

$$= \alpha \Delta t P_C(t). \quad (4)$$

In a similar way  $\text{Prob}[O \rightarrow C]$  can be found. Finally, the probability for a single ion channel to be open is:

$$\frac{dP_O}{dt} = \alpha(1 - P_O) - \beta(P_O) \quad (5)$$

Notice that the first term describes the process of being in the closed state and then moving to open, while the second term

<sup>3</sup>The consideration of a single ion channel corresponds to record a small patch in the membrane

<sup>4</sup>Information about more complicated schemes are given in Dayan et al. (1983) and in [Laing et al. (2010)].

considers the event of being in the open state and then closing the channel.

Some examples of this Markov process are shown in Fig. 3 (left hand side) assuming the rates  $\alpha$  and  $\beta$  as voltage independent. The probability of being in a closed or open state are plotted as function of time. By comparing open probabilities and dwell times in the three simulations, it is possible to see how transition probabilities in  $\alpha$  and  $\beta$  lead to distinct channel kinetics. It can be observed from the left, middle and bottom panels in Fig. 3 that while the relationship between  $\alpha$  and  $\beta$  is the same, the increase in fluctuations is considerable.

The key elements in Eq.(5) are the rates which generally are functions of the voltage  $\alpha = \alpha(V)$  and  $\beta = \beta(V)$ . The exact dependence has been obtain from experimental data. However, the general expression for these quantities can be obtain from thermodynamic arguments. Transitions involve the movement of an effective charge  $q \xi_{\alpha, \beta}$  through the potential  $V$  across the membrane ( $\xi_{\alpha, \beta}$  takes into account the amount of charge moved and the distance travelled). In addition, transitions described by the rates are likely to be limited by barriers requiring thermal energy [Dayan et al. (1983)]. Therefore, the probability that thermal fluctuations will provide enough energy to overcome this energy barrier is proportional to the Boltzmann factor  $\exp(-q \xi_{\alpha} V / K_B T)$ . Assuming these statements, and considering some constant  $A_{\alpha}$ , the form of  $\alpha$  can be expected as:

$$\alpha(V) = A_{\alpha} \exp(-q \xi_{\alpha} V / K_B T) = A_{\alpha} \exp(-\xi_{\alpha} V / V_T), \quad (6)$$

the expression for  $\beta$  should similar with its respective  $A_{\beta}$  and  $\xi_{\beta}$ .

### 2.4. Gillespie's method

Consider again a single two-state ion channel obeying the transition-state diagram (1). The probability that a single channel opens at time  $t$  remains closed until  $t + \tau$  is [Fall et al. (2002)]:

$$\text{Prob}(O, t + \tau | O, t) = \exp(-\beta\tau), \quad (7)$$

Where the open dwell time  $\tau_0$  of the channel is an exponentially distributed random variable RV. As it can be noticed the probability for a single channel to remain in its present state decreases exponentially with time. Therefore the corresponding probability distribution is:

$$\text{Prob}(\tau < \tau_0 \leq \tau + d\tau) = \beta \exp(-\beta\tau). \quad (8)$$

In this case, the analogous method to use a subroutine for simulating an exponentially distributed RV, is to choose a uniformly distributed RV "R" on the interval  $[0, 1]$  with the relation:

$$\tau_0 = \frac{1}{\beta} \ln(R) \quad \text{with } R \text{ on } [0, 1] \quad (9)$$

Fig. 3 (right hand side) shows examples of the two state model using this method, for the case of four ion channels ( $N=4$ ).

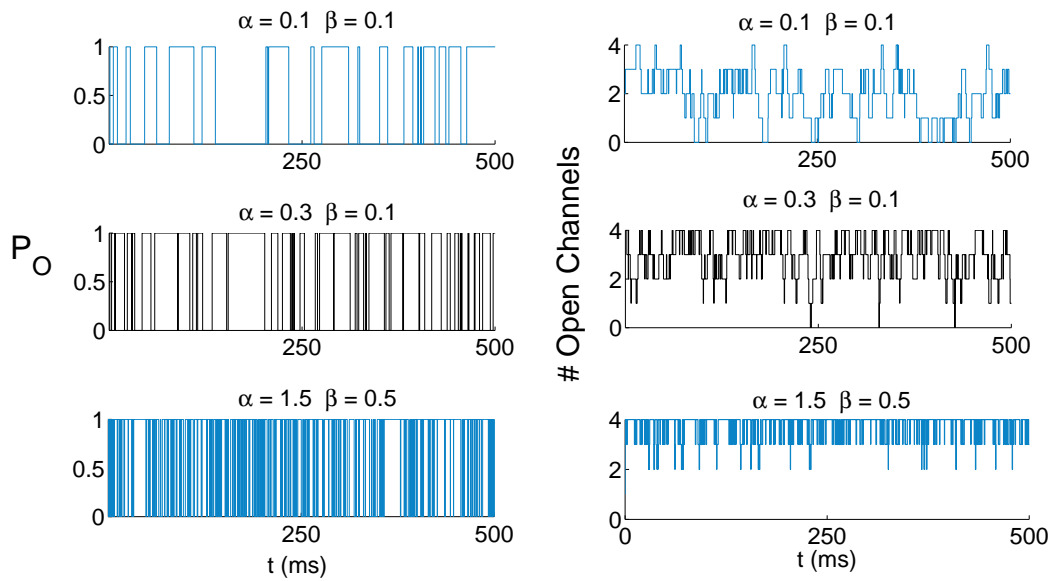


Figure 3: Left hand side: Monte Carlo simulation of the two state ion channel (closed-opened) for different rates. From top to middle figure, the gain rate ( $\alpha$ ) is increased three times, and from middle to bottom figure the gain and loss rate ( $\beta$ ) are increased by factor of five. Right hand side: Gillespie simulation for  $N = 4$  independent ion channels using the same rates applied for the Monte Carlo case.

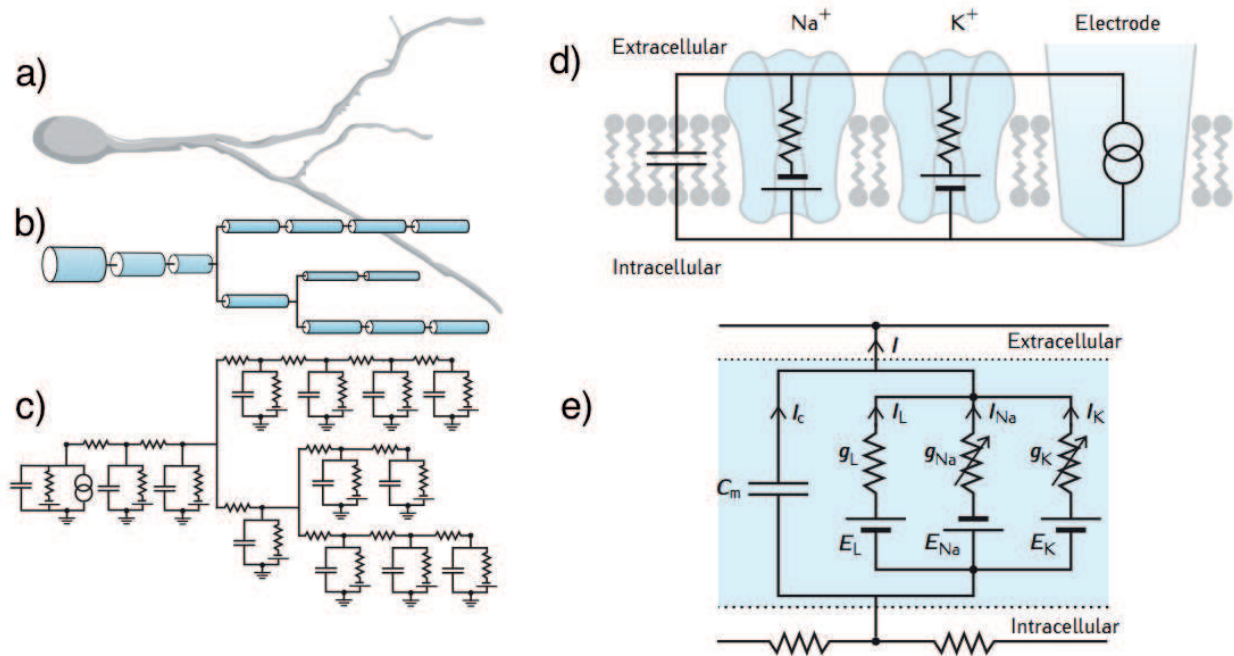


Figure 4: Left hand side, diagram of the development of a multi compartmental model: a) the cell morphology, b) representation of the neuron by a set of connected cylinders (the same geometrical figure is used to represent the soma and the branches), c) equivalent electrical circuit consisting of interconnected RC circuits (the only part of the neuron receiving current is the soma). Right hand side, circuit representation of the membrane: d) electrical circuit of a patch of membrane where an electrode is inserted inside the membrane, and e) the Hodgkin-Huxley electrical circuit containing the contribution of the current coming from different gating ion channels, the leak current, and the capacitive current. Figure taken from Sterrat et al. (2011): *Principles of Computational Modelling in Neuroscience*.

As it can be noticed with smaller rates, top panel, the number of open channels can go easily from 4 to 0 or vice versa. Furthermore, if the opening rate is increased the channels are rarely going to be completely closed. However, by looking at the bottom panel, if both rates are increased by three times, most of the time the channels are completely open.

For this project, the Gillespie method was used for two reasons: 1) it is much faster computationally than the Monte Carlo method and 2) the stochastic properties of individual ion channel states can be treated as statistically independent and memoryless RV and it is sufficient to track state occupancies for the whole population of ion channels. Therefore it is possible for the rates for all transitions to be determined within a single population of ion channels and to set how long the state of the population should persist.

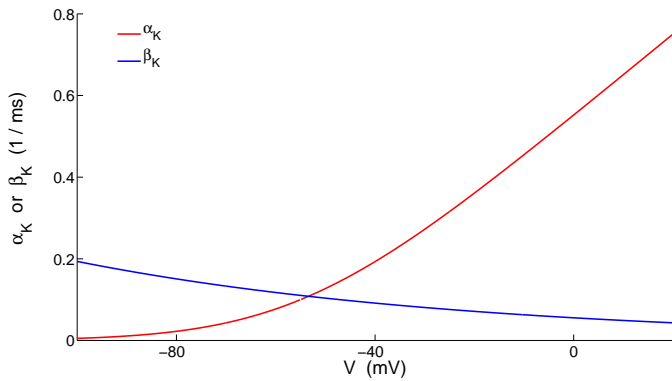


Figure 5: Voltage dependent gating functions  $\alpha_K(V)$  and  $\beta_K(V)$  of the Hodgkin Huxley model.

## 2.5. Compartmental model

The morphology of a cell can be represented by simple geometric figures such as spheres or cylinders. In the particular case of neurons, the soma is commonly represented by a sphere or cylinders, while dendrites and axons are represented as connected cylinders with different diameter [Sterratt et al. (2011)]. In general, dendrites cannot be treated as isopotential structures (which leads to axial current flowing along them), then in order to account for this in the model a single dendrite has to be represented as the connection of multiple compartments. Fig. 4 (a) and (b) respectively show how the discretization of the neuron can be performed, by presenting the cell morphology and the structure of interconnected cylinders. The soma corresponds to the wider cylinder and as long as we start moving away from it the cylinders are thinner. Additionally, Fig. 4 (b) shows that a single dendritic branch can be represented by connecting two or more cylinders.

Therefore, in compartmental modelling, the election of the size of the cylinders (being simulated in the dendritic tree of a neuron) is an important parameter in the model, i.e. the length  $l$  and a diameter  $d$ . For the case of a single compartment, this is treated as an isopotential entity, where the connection between compartments is treated by applying the correspondent

boundary conditions. The basis of modelling the electrical properties of a neuron is the resistorcapacitor electrical circuit (RC) consisting of a capacitor, leak resistor and a leak battery electrical circuit, i.e. this simple case represents a passive membrane. In order to calculate voltage changes in more than just an isolated region of membrane, it should be considered how the voltage spreads along the membrane. This can be modelled with multiple connected RC circuits. Fig. 4 (c) shows the diagram of a piece of neuron represented by a set of RC circuits connected in parallel. For this specific representation, the only part of the neuron receiving an applied current is the soma, then the structure of the diagram for the branches is equivalent.

Compartmental models are commonly used in computer simulations employing a finite number of compartments. It has been suggested that a certain amount of errors come from the inaccurate assumption of isopotential compartments [Sterratt et al. (2011)]. In practice it can be noticed that reducing the size of the used compartments reduces the amount of error but increases the number of sections required to represent the biological structure, consequently increasing the computational demand for the simulation.

## 2.6. Hodgkin Huxley model

In 1963, Andrew Fielding Huxley and Alan Lloyd Hodgkin proposed that changes in membrane permeability due to certain ions account for the observed changes in membrane voltage and that the potential tends to the Nernst potential<sup>5</sup> of the ion to which the membrane was mainly permeable [Laing et al. (2010)]. Using a voltage clamp<sup>6</sup> Hodgkin and Huxley demonstrated (1949) that both  $Na^+$  and  $K^+$  ions make important contributions to the ionic current during an action potential [Sterratt et al. (2011)], Fig. 4 (d) represents how using the voltage clamp technique a electrode (which is injecting current inside the membrane) is inserted inside the cell membrane and the corresponding RC circuit form by the electrode and the gating ion channels of  $Na^+$  and  $K^+$ .

Based on this assumption, Hodgkin and Huxley proposed an equivalent electrical circuit for a patch of nerve membrane with a capacitive current and ionic currents from the flow of  $Na^+$  ( $I_{Na}$ ) and  $K^+$  ( $I_K$ ) ions as well as a leak current ( $I_L$ ) (these currents are described in the following subsections). Fig. 4 (e) represents the diagram of the membrane made by Hodgkin and Huxley. Therefore to establish the differential equation satisfied by the voltage  $V$ , Kirchoff's law of charge conservation is applied to the circuit. This circuit can be described by

$$C \frac{dV}{dt} + I_{ions} = I_{app} \quad (10)$$

where

$$I_{ions} = I_{Na} + I_K + I_L \quad (11)$$

<sup>5</sup>Nernst potential is the equilibrium potential, where the electrical and osmotic forces are balanced for a particular type of ion.

<sup>6</sup>The voltage clamp was introduced by Cole and Marmount and is used in electrophysiology to measure ionic currents across cell membranes at fixed voltages.

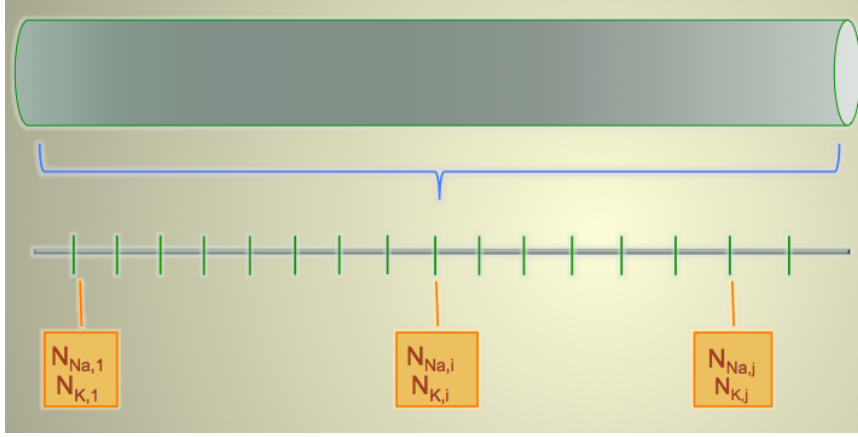


Figure 6: Localization of clusters along the dendrite. A single compartment was mapped into a finite line where equally separated clusters were located. Each cluster contains a different  $N_{Na,i}$  and  $N_{K,i}$  number of ion channels.

with  $I_{app}$  the current applied through experimental manipulation and  $C$  the membrane capacitance.

The Hodgkin Huxley model also describes how the action potential propagates along structures like axons and dendrites. In a continuous cable model, the contribution due to the length of the cable is the second derivative of the membrane potential with respect to space. The equation that describes the behaviour of voltage in a single compartment has the form of a model is reaction diffusion equation:

$$\frac{\partial V}{\partial t} = D \frac{\partial^2 V}{\partial x^2} + \frac{V - E_L}{\tau} - \frac{1}{\pi a C} \sum_{i,n} \delta(x - x_n) I_{i,n}(t), \quad (12)$$

where  $0 \leq x \leq L$ . The index  $n$  is used for labelling different positions along the cable and  $i$  index describes the contribution of currents coming from different gating ion channels and the diffusion term is given by  $D_j$  whose expression depends on the electrotonic space constant  $\lambda$  and in the membrane time constant  $\tau$  as

$$D_j = \lambda_j^2 / \tau$$

where

$$\lambda_j = \sqrt{a_j R / (4R_a)} \quad \text{and} \quad \tau = C R.$$

The magnitude of each type of ionic current is calculated from the product of the ions driving force<sup>7</sup> and the membrane conductance  $g_i$  for a specific ion:  $I_{ij} = g_i(V_j - E_i)$  where  $E_i$  describes the corresponding equilibrium potential. In particular

$$\begin{aligned} I_{Na} &= g_{Na}(V - E_{Na}), \\ I_K &= g_K(V - E_K), \\ I_L &= \bar{g}_L(V - E_L), \end{aligned}$$

are used in this work.

<sup>7</sup>The driving force corresponds to the difference between the voltage applied and the voltage at which there is no flow (Nernst potential)

## 2.7. Leakage current

The leakage current (leak current), is created by resting channels, which are permanently open, and they are responsible for generating the resting membrane potential. In most kind of neurons, resting channels are mainly permeable to chloride ( $Cl^-$ ) ions and the remaining channels are permeable to  $K^+$  and  $Na^+$ . The current created by these channels has the capacity of persist throughout changes in membrane potential as depolarization (increase in voltage).

## 2.8. Sodium current

The sodium resting potential is around 50 mV, and the extracellular concentration of sodium ions is greater than inside the cell. For membranes of different cells, Na channels work as pacemakers or contribute to creating the threshold potential that underlies the decision to fire or not to fire [Sterrat et al. (2011)]. For this particular kind of ion channel, the voltage dependence for the opening  $\alpha_{Na}$  and closing  $\beta_{Na}$  rates are given by

$$\alpha_{Na} = \frac{0.1(V + 40)}{1 - \exp(-0.1(V + 40))} \quad (13)$$

$$\beta_{Na} = 4 \exp(-0.556(V + 65)) \quad (14)$$

When current is injected in the cell it can increase the membrane potential (which implies in the Hodgkin Huxley model to add the contribution of a term related to positive current). When this current drives the membrane potential up to  $-50$  mV, the  $\alpha_{Na}$  variable jumps from a value near to zero to almost one, this causes a large flux of  $Na^+$  ions to enter the membrane rapidly raising the potential to around 50 mV (the sodium resting potential) producing the large spike in voltage that characterizes the action potential. The rise in membrane potential causes the  $Na^+$  conductance to inactivate, then the correspondent  $Na^+$  current is shut off.

## 2.9. Potassium current

The potassium resting potential is around  $-77$  mV and the concentration of  $K^+$  inside the cell is greater than the external concentration and when the neuron tends to increase the

	Nomenclature	Parameter	Units
Diffusion coefficient	D	2.5E4	$\mu m^2 ms^{-1}$
Membrane time constant	$\tau$	3.3	$ms$
Membrane capacitance	C	1	$\mu F cm^{-2}$
Branch length	L	100	$\mu m$
Branch diameter	a	1	$\mu m$
Na reversal potential	$E_{Na}$	50	$mV$
K reversal potential	$E_K$	-77	$mV$
Leak reversal potential	$E_L$	-70	$mV$
Na conductance	$g_{Na}$	20	$pS$
K conductance	$g_K$	20	$pS$

Table 1: Parameter set used in the model of a single dendrite.

membrane voltage, potassium channels allow ions to exit the cell in order to make the interior more negative and reestablish the equilibrium potential (membrane potential) which in non-exitable conditions is around  $-70$  mV. Furthermore, when the neuron is set at the threshold potential<sup>8</sup>  $K^+$  channels control the duration of the spikes keeping the lasting time short [Hille et al. (2001)]. In addition, these kinds of channel are capable of terminating periods of intense activity and timing the intervals between firing. The voltage dependance for the opening  $\alpha_K$  and closing  $\beta_K$  rates for this kind of channels are given by

$$\alpha_K = \frac{0.01(V + 55)}{1 - \exp(-0.1(V + 55))} \quad (15)$$

$$\beta_K = 0.125 \exp(-0.0125(V + 65)) \quad (16)$$

where  $V$  is expressed in mV. Figure. 5, shows the exponential decay of  $\beta_K = \beta_K(V)$  and the exponential grow  $\alpha_K = \alpha_K(V)$  as the voltage is going close to zero.

### 2.10. Parameters

For the purpose of this work, a single compartment was mapped into a finite line where equally separated clusters were located. Each cluster contains a group of  $Na^+$  and a group of  $K^+$  gating ion channels modelled with Gillespie method. It has been found that the average density of  $Na^+$  channels along dendrites is  $60 \times 10^8$  channels per  $cm^2$ , and the average density of  $K^+$  channels is  $18 \times 10^8$ . Therefore, corresponding with the diameter and length of the compartment used, see (Table 1), the number of  $Na^+$  and  $K^+$  channels used was 6000 and 1800 respectively. These channels were randomly distributed along the line that represents the compartment and then located into the nearest cluster. Therefore  $x_n$  in Eq. (12) corresponds to the location of the different clusters. Fig. 6 shows how the clusters where located into the dendrite.

Suppose that  $N$  clusters where used, then the number of groups of gating ion channels is  $2N$ . According to Gillespie

<sup>8</sup>The threshold potential is the critical level to which the membrane potential has been depolarized in order to initiate an action potential (it triggers the nerve impulse). The common value of this potential is between  $-50$  to  $40$  mV.

each group is going to change the number of open ion channels (opening or closing a single one) in a time  $\tau_j$  with  $j \in [1, 2N]$ . However, the clusters are constrained to be in the cable, so they can change their state independently from the neighbouring clusters. In addition, the way in which these gating channels are going to contribute to modify the total voltage  $V$  is given by Eq. 12 (which is a partial differential equation (PDE)), and in order to numerically solve this PDE the time step ( $dt$ ) has to be fixed. Therefore the time step give by Gillespie cannot be used to evolve the diffusion equation. Nonetheless, through the use of the Gillespie model, the minimum time  $dt'$  in which an event can happen (opening or closing one channel) can be known. Hence, the PDE is evolve using a fixed  $dt$  where  $dt < dt'$ , and once  $dt$  reaches the value of  $dt'$ , the times  $\tau_j$  are calculated. If  $\tau_j \leq dt'$ , the corresponding group of ion channels is going to actualize to a new state.

The fact that in general  $dt < dt'$  comes from the fact that Eq. (12) that has to be solved is a reaction diffusion equation. In order to numerically solve these kind of equations, the Courant Friedrichs Lewy (CFL) condition has to be taken into account. The CFL condition is required for convergence when a hyperbolic partial differential equation is trying to be solved by the method of finite differences Sauer et al. (2006) and involves a relationship between the diffusion constant  $D$ , the time step  $dt$  and the spatial step  $dx$  of the PDE

$$D \frac{dt}{(dx)^2} < \frac{1}{2}. \quad (17)$$

In addition the PDE was solved using a Runge-Kutta method of order four (RK4). The convergence properties of a fourth order method like RK4, are higher than those of orders 1 and 2 such as the Euler and Trapezoid methods respectively. Convergence here means, how fast the error of the ODE approximation at time  $t$  goes to zero as the step size  $dt$  goes to zero. Fourth order implies that for every halving of the step size, the error drops by approximately a factor of  $2^4$ . Then the voltage in Eq. (12) was discretized and calculated as

$$V_{i+1} = V_i + \frac{dt}{6}(s_1 + 2s_2 + 2s_3 + s_4) \quad (18)$$

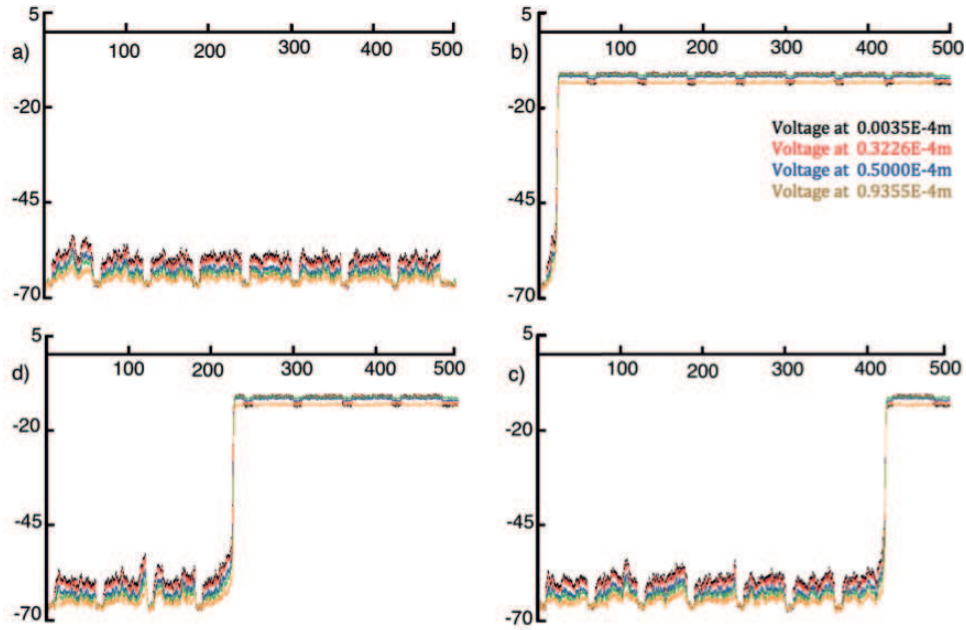


Figure 7: Voltage recordings of 500ms made for specific sections of a dendrite of length  $100\mu\text{m}$  ( $1E - 4\text{m}$ ). For this graphs  $g_{leak} = 0.026\text{cm}^2/\text{S}$ . Panel (a) shows fluctuations in voltage due to the random transitions between open and close states of the gating ion channels. From (b-d) shift of the voltage membrane due to a threshold voltage is reach that leads a fast increase on it. In black colour is presented the point of the injection current ( $0.0035E - 4\text{m}$ ) away from the beginning of the dendrite. In red colour is plotted the voltage associated with the nearest cluster to the current injection ( $0.0645E - 4\text{m}$ ), in blue colour is presented the voltage of an intermediate cluster between the beginning and the middle point of the dendrite ( $0.3226E - 4\text{m}$ ). Green colour corresponds to the middle section of the dendrite ( $0.56E - 4\text{m}$ ), and yellow colour represents one of the clusters almost at the end of the cable ( $0.9355E - 4\text{m}$ ).

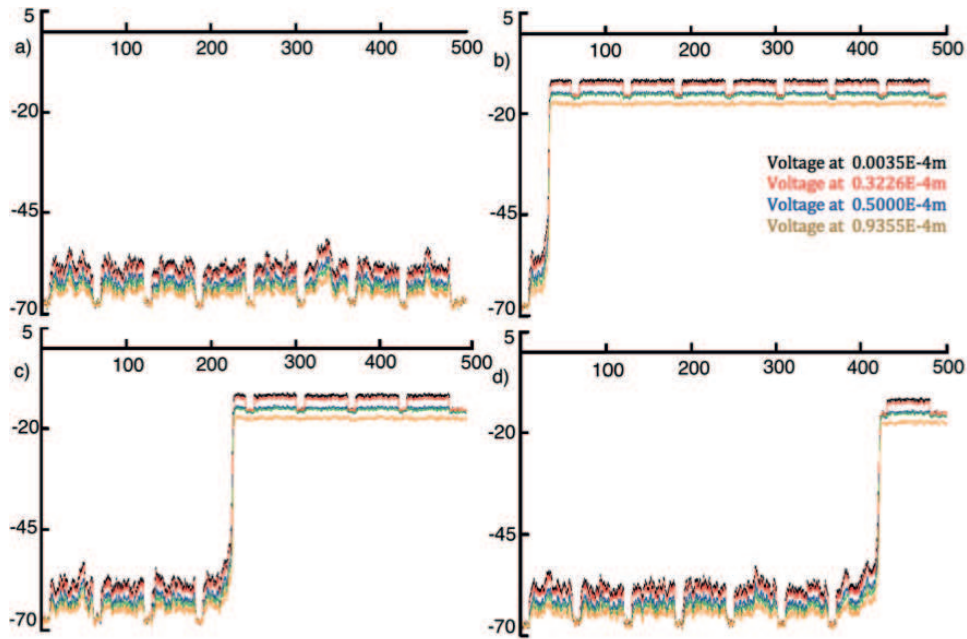


Figure 8: Voltage recordings of 500ms made for specific sections of a dendrite of length  $100\mu\text{m}$  ( $1E - 4\text{m}$ ). For this graphs  $g_{leak} = 0.0144\text{m}^2/\text{S}$ . Panel (a) shows fluctuations in voltage due to the random transitions between open and close states of the gating ion channels. From (b-d) shift of the voltage membrane due to a threshold voltage is reach that leads a fast increase on it. In black colour is presented the point of the injection current ( $0.0035E - 4\text{m}$ ) away from the beginning of the dendrite. In red colour is plotted the voltage associated with the nearest cluster to the current injection ( $0.0645E - 4\text{m}$ ), in blue colour is presented the voltage of an intermediate cluster between the beginning and the middle point of the dendrite ( $0.3226E - 4\text{m}$ ). Green colour corresponds to the middle section of the dendrite ( $0.56E - 4\text{m}$ ), and yellow colour represents one of the clusters almost at the end of the cable ( $0.9355E - 4\text{m}$ ).



and

$$\begin{aligned}
s_1 &= f(t_i, V_i), \\
s_2 &= f\left(t_i + \frac{dt}{2}, V_i + \frac{h}{2}s_1\right), \\
s_3 &= f\left(t_i + \frac{dt}{2}, V_i + \frac{h}{2}s_2\right), \\
s_4 &= f\left(t_i + \frac{dt}{2}, V_i + hs_3\right),
\end{aligned}$$

where  $f(t_i, V_i)$  is the expression in the right hand side of Eq. (12).

### 3. Results

A dendrite of  $100\mu m$  of length and diameter  $1\mu m$  was modelled, locating on it thirty clusters. Each cluster contained on average 200  $Na^+$  and 60  $K^+$  ion channels. At the beginning of the dendrite a trend of nine identically square pulses of current was applied. The amplitude of each pulse was  $0.1 nA$  with a duration of  $50 ms$  and a delay of  $10 ms$ . Recordings of the activity of the neuron were made for  $500 ms$ .

Fig. 7 and Fig. 8 present the recordings made for specific sections of the dendrite. For an easy description the longitude of the dendrite (cable) is going to be considered as  $1E - 4m$  and the starting point of the dendrite is zero metres. Then the longitude of the dendrite is measured from 0 to  $1E - 4m$ . In all the panels of these two figures, with black representing the location of the point of the current injection,  $0.0035E - 4m$ , red represents the response of the nearest cluster of gating ion channels located  $0.0645E - 4m$  away from the beginning of the dendrite, purple, the response of a cluster relatively more separated of the point of current injection  $0.32E - 4m$ , green, is the middle point of the dendrite  $0.50E - 4m$  and orange represents the activity of one of the clusters almost in the end of the cable.

The initial condition for the (12) was a flat  $-70mV$ , and the value of  $g_{leak}$  was  $0.026cm^2/S$ . In Fig. 7 (a) the fluctuations on voltage the cable are presented. These fluctuations are consequence of the current applied (the bigger fluctuations appear in the times when the current is switched on) and the stochastic gating of the ions contained in the clusters. Notice that the spontaneous fluctuations in voltage can achieve values nearing  $-50mV$ . What is also important to note is the visible presence of diffusion in the voltage equation, as for the nearest points to the injection current the voltage is slightly greater than for points nearing the end of the dendrite. For the case of Fig. 7 (b), for the same initial conditions that in Fig. 7 (a), a large fluctuation changed the whole set of plots in a neighbourhood of  $-10mV$ , and for the rest of the time the voltage never returns to a region close to the initial condition. However small changes in voltage are still visible in the top of the figure, but these fluctuations in the points of applied current are smaller than the ones found in Fig. 7 (a). In addition, the

presence of the diffusion factor is still evident as for the points near the beginning of the dendrite the square shape of the voltage (due to the square pulse of current) is clearly visible, but for points away from the injection current this square shape is not clearly visible.

The presence of this shift in voltage can be found at any time in the recording of the voltage (between 0 and  $500 ms$ ). Two more examples of this behaviour of the shift in voltage are shown in Fig. 7 (c) and Fig. 7 (d). For the first one, the shift appears after  $200 ms$  of being recording the voltage while in the second one, the shift comes out just after  $450 ms$ . Notice that in the time between zero and the time just before the shift, the bigger fluctuations that came along Fig. 7 (a) are also appearing. In order to see the dependence of the voltage on the dendrite as function of the number of clusters, we remove half of them from the cable, maintaining in the remaining clusters exactly the same number of  $K^+$  and  $Na^+$  gating ion channels as in Fig. 7. The simulation was run taking the same initial conditions as in the previously described figure (initial voltage  $-70mV$  and  $g_{leak} = 0.026cm^2/S$ ). For this case, it was found that the fluctuations in voltage are considerably smaller than for the case of 30 clusters. As a consequence of this, the shift in voltage is never found. In the other hand, diffusion is still present and it seems to quickly reduce the current injected at the beginning of the dendrite.

Considering the case of 15 clusters, we change the initial conditions, of the (12), taking now the value of  $g_{leak}$  as  $0.0144cm^2/S$  and maintaining the initial voltage in  $-70 mV$ , the big fluctuations in voltage are found again Fig. 8 (a). In addition the shift in voltage randomly appears again. Fig. 8 (b) presents the big change in voltage at the beginning of the simulation. What is remarkable of this figure is that the effects of diffusion are greater, because for the blue line (position  $0.32E - 4m$  in the cable), the current applied seems to almost disappear. An effect that is clear at the end of the cable (yellow line). Moreover, Fig. 8 (c) and Fig. 8 (d) show examples of the big change in voltage for different times, the behaviour of diffusion is same as the one describe for Fig. 8 (b). The effect of the big change in voltage was seen for the particular parameters describe in the previous section. For Fig. 7 and Fig. 8, we tried to modified the characteristics of the pulse of current that was applied, changing the delay or duration but always maintaining the same amplitude<sup>9</sup>. The results, were the same that the ones presented in Fig. 7 and Fig. 8, because the shift in voltage appeared randomly in the points where current was applied.

<sup>9</sup>The amplitude was not changed, as it is known that a big pulse corresponds with a faster opening of the gating channels.

## 4. Discussion

The results shown in the last section clearly demonstrate the stochastic behaviour of the gating ion channels. The particular values of  $g_{leak}$  for which a random shift in voltage occurs were found by manually changing this parameter and looking at the global behaviour. In addition, for this specific values of  $g_{leak}$ , the system seems to be describing an unstable point, because if the value of  $g_{leak}$  is modified (increase or decrease) the fluctuations rapidly disappear.

The fluctuations in voltage that appeared in Fig. 7 and Fig. 8 are due to stochastic opening and closing changes of the states of the gating ion channels. When this fluctuations reach a threshold value, the shift in voltage occurs. The value of this threshold for all the figures shown in this work is around  $-45$  mV. The fact that once the shift occurs the voltage never returns to its initial value is mainly because after the shift occurs current is still being applied.

For the two cases presented, using 30 and 15 clusters the results are mainly the same, the differences found were: 1) The specific value of  $g_{leak}$  were the fluctuations and the shift in voltage occurs in a randomly way (all along the time of the voltage recording) are not the same, and 2) the consequences of diffusion are bigger for the case when 15 clusters were taking into account<sup>10</sup>.

## 5. Conclusion

In this work we discussed the importance of stochastic gating ion channels in nervous cells and show how this kind of ion channels may be modelled as a Markov process. The concept of gating ion channels was firstly introduced, together with the description of a simple kinetic scheme of two states for the channels: open and closed states. It was also shown how the probability of being in either one of the two states can be calculated. Finally, we present discussion on how Gillespie's method improves the numerical simulation over the traditional Montecarlo simulation.

In addition, we show how the neurons can be discretized by using geometrical figures and then model them as multiple connected RC circuits. Furthermore, the Hodgkin Huxley model was used in order to introduce the equation that describes the propagation of the action potential along like-dendritic structures. The circuit model of the dendrites and the types of currents that contribute to increase or decrease the membrane potential was further treated.

Finally, we present some plots which show how the stochastic behaviour of the ion channels affects the voltage in the membrane; a proof of this is that subject to an applied current, the

<sup>10</sup>For more information about Markov process applied to gating ion channels check: Kamran et al. (2006) and Schmandt et al. (2012).

ion channels generate fluctuations on the voltage membrane, and because of this, it is shifted to a new voltage state with a higher value. This shift, for specific biological parameters, can randomly occur during the voltage recording along the cable. The effect of diffusion can also be appreciated. This effect strongly suggests that the compartment should not be treated as an isopotential entity, for the pulse injected in the beginning of the dendrite is not entirely recovered at its final position.

## Further Work

In this project gating ion channels were modelled by a specific Markov chain model, the simplest model in this class: two transition states (open and closed). Most Markov chain models of ion channel gating are more complex than the two-state model to include multiple closed and/or open states as well as voltage-dependent transitions. Therefore we will intend to account for this.

## 6. Acknowledgement

I would like to thank my advisors, Prof. Yulia Timofeeva and Prof. Michael Tildesley for their valuable comments and help during the development of this project, for the time they dedicated whenever I had some questions and overall for their friendship and their patience. Finally, I would like to acknowledge the Erasmus Mundus Consortium for allowing me both the opportunity and the resources to get closer to my personal and academic goals by joining me to the M.S. in Complexity Science programme.

## References

- Kandel E, Schwartz J, Jessell (2012) Principles of Neural Science. McGraw-Hill Medica, New York.
- Masukawa L, Prince D (1983) Synaptic Control of Excitability in Isolated Dendrites of Hippocampal Neurons. The Journal of Neuroscience. Vol 4, No 1, pp. 217-227.
- Koch C, (1999) Biophysics of Computation. Oxford University Press. New York.
- Dayan P, Abbott L (1983) Theoretical Neuroscience: Computational and Mathematical Modeling of Neural Systems. The MIT Press. Massachusetts.
- Fall C, Marland E, Wagner J, Tyson J (2002) Computational Cell Biology. Springer-Verlag, New York.
- Strassberg A, DeFelice L (1993) Limitations of the Hodgkin-Huxley Formalism: Effects of Single Channel Kinetics on Transmembrane Voltage Dynamics. Neural Computation, Vol. 5 p843-855.
- Cannon R, O'Donnell C, Nolan M (2010) Stochastic Ion Channel Gating in Dendritic Neurons: Morphology Dependence and Probabilistic Synaptic Activation of Dendritic Spikes. PLoS Comput Biol 6(8): e1000886.
- Hille B (2001) Ion Channels of Excitable Membranes. Sinauer Associates, Massachusetts.
- Yuan L, Chen X, (2005) Diversity of Potassium Channels in Neuronal Dendrites. Elsevier, Progress in Neurobiology 78, 374-389.
- Serrat D, Graham B, Gillies A, Willshaw D (2011) Principles of Computational Modelling in Neuroscience. Cambridge University Press, New York.
- Schmandt N, Galan R (2012) Stochastic-Shielding Approximation of Markov Chains and its Application to Efficiently Simulate Random Ion Channel Gating. Physical Review Letters, 109-118101.
- Kamran D, Koch C, Segev I (2006) Spike propagation in dendrites with stochastic ion channels. Journal of Computational Neurosciences, 20: 77-84.
- Laing C, Lord G, (2010) Principles of Computational Modelling in Neuroscience. Oxford University Press, New York.
- Sauer T (2006) Numerical Analysis. Pearson Education, Boston.